Chapter 7

Exploring and Using the Magnetic Methods

Othniel K. Likkason

Additional information is available at the end of the chapter

http://dx.doi.org/10.5772/57163

1. Introduction

The Earth is principally made up of three parts: core, mantle and crust (Fig. 1). As understood today, right at the heart of the Earth is a solid inner core composed primarily of iron. At 5, 700°C, this iron is as hot as the Sun's surface, but the crushing pressure caused by gravity prevents it from becoming liquid. Surrounding this is the outer core, a nearly 2, 000 km thick layer of iron, nickel, and small quantities of other metals. Lower pressure than the inner core means the metal here is fluid. Differences in temperature, pressure and composition within the outer core cause convection currents in the molten metal as cool, dense matter sinks while warm, less dense matter rises. This flow of liquid iron generates electric currents, which in turn produce magnetic fields (Earth's field). These convection processes in the liquid part of core (outer core) give rise to a dipolar geomagnetic field that resembles that of a large bar magnet aligned approximately along the Earth's rotational axis. The mantle plays little part in the Earth's magnetism, while interaction of the past and present geomagnetic field with the rocks of the crust produces magnetic anomalies recorded in detailed when surveys are carried out on or above the Earth's surface.

The magnitude of the Earth's magnetic field averages to about $5x10^{-5}$ T (50, 000 nT). Magnetic anomalies as small as 0.1 nT can be measured in continental magnetic surveys and may be of geological significance.

The magnetic methods, perhaps the oldest of geophysical exploration techniques bloomed after the World War II. Today, with improvements in instrumentation, navigation and platform compensation, it is possible to map the entire crustal section at a variety of scales from strongly magnetic basement at a very large scale to weakly magnetic sedimentary contacts at small scale. Methods of magnetic data treatment, filtering, display and interpretation have also advanced especially with the advent of high performance computers and colour raster graphics.

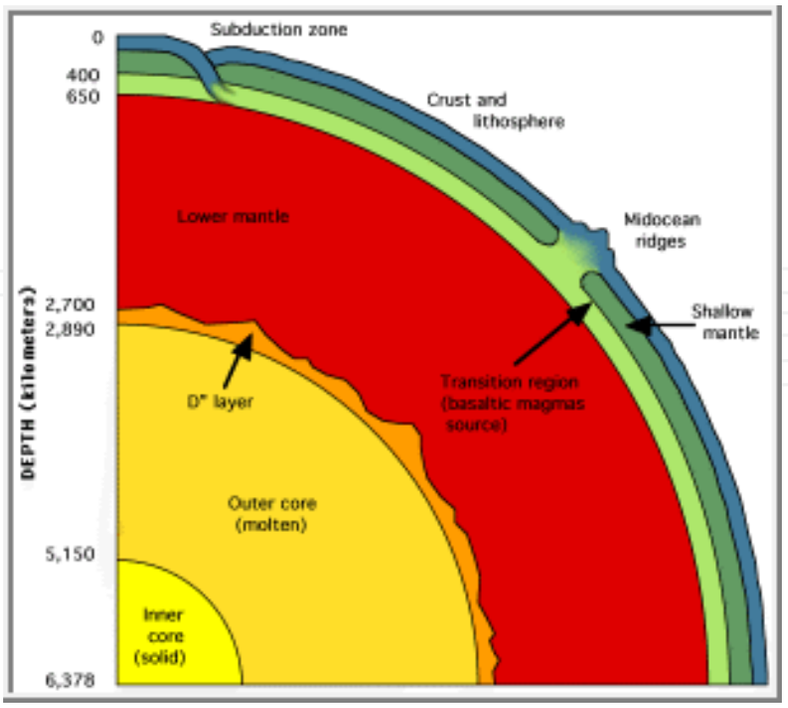

Figure 1. Internal structure of the Earth (from http://zebu.uoregon.edu)

As is well known today, magnetic methods are used to solve various problems such as:

1. Mapping the basement surface and sediments in oil/gas exploration
2. Detecting different types of ore bodies in mining prospecting
3. Detecting metal objects in engineering geophysics
4. Mapping basement faults and fractures
5. Determining zones with different mineralization in logging as well as inspecting casing parameters
6. Studying the magnetic field of the Earth and its generators and
7. A variety of other purposes such as natural hazards assessment, mapping impact structures and environmental studies.

Magnetic observations are obtained relatively easily and cheaply and a few corrections are applied to them. This explains why the magnetic methods are one of the most commonly used geophysical tools. Despite these obvious advantages, interpretations of magnetic observations suffer from a lack of uniqueness due to dipolar nature of the field and other various polarization effects. Geologic constraints, however, can considerably reduce the level of ambiguity. Information from magnetic surveys comes from rock units at depth as well as from those at or near the surface. This is the strength of the magnetic method (or any surface geophysical method), making it more powerful than any other remote sensing method which relies on the information from reflections of electromagnetic (EM) waves by materials on the Earth surface.

http://dx.doi.org/10.5772/57163

Thus while the natural magnetic field of the Earth is measured in magnetic method, EM radiation normally is used as the information carrier in remote sensing. Electromagnetic radiation is a form of energy with the properties of a wave, and its major source is the sun. Solar energy traveling in the form of waves at the speed of light is known as the electromagnetic spectrum. Passive remote sensing systems record the reflected energy of electromagnetic radiation or the emitted energy from the Earth, such as cameras and thermal infrared detectors. Active remote sensing systems send out their own energy and record the reflected portion of that energy from the Earth's surface, such as radar imaging systems.

In this chapter, we explore the magnetic methods of geophysical exploration. The first part of the chapter covers the fundamental concepts of magnetic force field, the Earth's magnetic field and its relationship with gravity field. The second part deals with the measurement procedures and treatment of the magnetic field data, while the third part covers the magnetic effects of simple geometric bodies, processing and interpretation of magnetic data and ending it with treatment, analysis and interpretation of real field data.

2. Fundamental magnetic theories

Any magnetic grain is a dipole. That is, it has two poles, P_1 and P_2 of opposite signs diametrically linked. Charles Augustin de Coulomb in 1785 showed that the force of attraction or repulsion between electrically charged bodies and between magnetic poles obeys an inverse square law similar to that derived for gravity by Newton.

The mathematical expression for the magnetic force, F_m experienced between two magnetic monopoles is given by:

$$F_m = \frac{1}{\mu}\frac{P_1 P_2}{r^2} \tag{1}$$

Where μ is a constant of proportionality known as the magnetic permeability, P_1 and P_2 are the 'strengths' of the magnetic monopoles and r is the distance between the poles.

We note that the expression in equation (1) is identical to the gravitational force, $F_g = G\frac{m_1 m_2}{r^2}$ and electrical force, $F_g = k\frac{q_1 q_2}{r^2}$ expressions. Here m_1, m_2 and q_1, q_2 are respectively masses and electrical charges separated by distance r, G is the universal gravitational constant while k is the Coulomb's law constant for the medium. However, unlike the gravitational constant, G, the magnetic permeability, μ is a property of the material medium in which the two monopoles, P_1 and P_2 are situated. If they are placed in a vacuum, then μ is for the free space. Also, unlike m_1 and m_2, P_1 and P_2 can be either positive or negative in sign. If P_1 and P_2 have the same sign, the force, F_m between the two monopoles is repulsive. If P_1 and P_2 have opposite signs, F_m is attractive.

We may seem to easily compare the gravitational force between masses m_1 and m_2 separated by r to that of either the attractive or repulsive magnetic force between two monopoles.

However, the magnetic monopoles have never existed! Rather the fundamental magnetic element appears to consist of two magnetic monopoles: one positive and the other negative, separated by a distance. Thus the fundamental magnetic element consisting of two monopoles is called a magnetic dipole. Every magnetic grain is therefore a dipole.

We can therefore determine the force produced by a dipole by considering a force produced by two monopoles. Since the dipole is simply two monopoles, each of strength P_1 and P_2, we expect that the force generated by a dipole is simply the force generated by one monopole added vectorially to the force generated by the second monopole. Consequently, the force distribution for a dipole is nothing more than the magnetic force distribution observed around a simple bar magnet. Thus a bar magnet can be thought as two magnetic monopoles separated by a length of the magnet. The magnetic force appears to originate out of the North Pole (N) of the magnet and to terminate at the South Pole (S) of the magnet. Some of the field lines pass through the material of the magnet (high concentration because of high μ), some pass through air (low concentration because of low μ). Notice that even in air; the poles have high density of field lines. Also, the lines radiate out from N (vertically outward) and radiate into S (vertically inward). Between the length of the bar in air, the magnetic field directions are variable, but with the middle of the bar having a near horizontal field direction. Again, the field strength and direction at any point around the bar magnet is a vector sum of the force field contributed by each of the monopole (N or S).

When we examine equation (1) in terms of unit of measurement, we see that the magnetic force, F_m retains its fundamental unit of newton (N) and r^2 would be in square metre (m^2). Permeability, μ by the S. I. unit definition, is a unitless constant. The units of the pole strength, P are defined such that if a force of 1 N is produced by two unit poles separated by a distance of 1 m, then each unit pole has a strength of one ampere-metre (1 Am). Thus a unit pole has an S.I unit of ampere-metre.

We can also define, from equation (1), the force per unit pole strength exerted by a magnetic monopole, P_1 or P_2. This is called magnetic field strength or magnetizing force, H. Thus

$$H = \frac{F_m}{P_2} = \frac{P_1}{\mu r^2} \tag{2}$$

Here again, given the units associated with force (N) and magnetic monopoles (Am), the unit associated with magnetic field strength, H are N/A-m and by definition, 1 N/A-m is referred to as a tesla (T): named after a Croatian inventor, Nikola Tesla. Thus 1 T = 1 N/Am. Indeed from equation (2), the unit of H can be expressed as Am/m^2 or Am^{-1} (ampere per metre). Thus 1 N/Am = 1 Am^{-1} = 1 T. Similarly, the unit of magnetic flux is weber (Wb) and magnetic flux per unit area is the magnetic strength we have been talking about. Thus the unit of magnetic strength can also be expressed in weber per square metre (Wb/m^2). Hence 1 Wb/m^2 = 1 T.

When describing the magnetic field of the Earth, it is common to use units of nanotesla (nT), where 1 nT = 10^{-9} T. The average strength of the Earth's magnetic field, H is about 50, 000 nT (ranges from 20, 000 to 70, 000 nT). A nanotesla has the value as the old unit of gamma (1 nT = 1 gamma).

When magnetic materials or rocks are placed within a field, T (a magnetizing force such as H given in equation (2)), the magnetic materials or rocks will produce their own magnetizations or polarizations. This phenomenon is called induced magnetization, magnetic polarization or magnetic induction. The strength of the magnetic field induced on the magnetic material due to the inducing field, T is called the intensity of magnetization or magnetic polarization, J_i; where

$$J_i = kT \tag{3}$$

The constant of proportionality, k is the magnetic susceptibility and is a unitless constant determined by the physical properties of the magnetic material. The susceptibility, k can either be positive or negative in values. Positive values imply that the field, J_i is in the same direction as the inducing field T. Negative k implies that the induced magnetic field is in the opposite direction as the inducing field. Details of the mechanisms of induced magnetization can be further obtained from [1].

In magnetic exploration method, the susceptibility is the fundamental material property whose spatial distribution, we attempt to determine. We see that magnetic susceptibility is analogous to density in gravity surveying. Unlike density, there is a large range of susceptibilities even within materials and rocks of the same type. This definitely will put limit to knowledge of rock type through susceptibility mapping of an area.

Magnetic susceptibility in SI unit is a dimensionless ratio having a magnitude much less than 1 for most rocks. Hence a typical susceptibility value may be expressed (as for example) k = 0.0064 SI. In the old c.g.s. system of electromagnetic units (emu), the numerical value of magnetic susceptibility for a given specimen is smaller by a factor of 4π than the SI value. Thus k (SI) = k (emu) x 4π. Hence for k = 0.0064 SI, k (emu) = k (SI)/4π = 0.00051 emu.

3. The Earth's magnetic field

Nearly 90% of the Earth's magnetic field (geomagnetic field) looks like a magnetic field that would be generated from a dipolar magnetic source located at the centre of the Earth and nearly aligned with the Earth's rotational axis. This field is believed to originate from convection of liquid iron in the Earth's outer core [2] and is monitored and studied using global network of magnetic observatories and various satellite magnetic surveys. If this dipolar description of the Earth's field were complete, then the magnetic equator would nearly correspond to the Earth's geographic equator and the magnetic poles would also nearly correspond to the geographic poles. The strength of the Earth's field at the poles is about 60, 000 nT. This is called the Main Field of the Earth. This field changes slowly with time and is believed to go through a decay and collapse, followed by polar reversal on a time scale of the order of 100, 000 years [3], [4]. The construction of a global magnetic reversal timescale is of fundamental importance in deciphering Earth's history. For details on such discussion, [5] can be consulted.

The remaining 10% of the Earth's magnetic field cannot be explained in terms of simple dipolar sources. The larger component of this 10% of the Earth's field originates in iron-bearing rocks near the Earth's surface where temperatures are sufficiently low (i.e. less than the Curie temperature of the rocks). This region is confined to the upper 30 – 40 km of the crust and is the source of the crustal field which is made up of induced field on magnetically susceptible rocks and remanent magnetism of the rocks. The smaller portion of the 10% comes from the upper atmosphere (external source).

The external source field is believed to be produced by interactions of the Earth's ionosphere with the solar wind. Hence some temporal variations (usually variable over hours at tens of nT or occasionally variable over a few hours at hundreds of nT: the magnetic storm) are correlated to solar activity. The external component (except for magnetic storm phenomenon) is usually regular and are corrected/removed appropriately from field measurements in a process similar to drift correction in gravity surveys. Where magnetic storm is detected, survey is most often discontinued until after the phenomenon has passed.

The crustal field, its relation to the distribution of magnetic minerals within the crust, and the information this relation provides about exploration targets are the primary subjects of the magnetic method in exploration. In a magnetic survey, the magnetic induction, B whose magnitude is measured at a point is the vector sum of four field components:

1. The Earth's **main field** which originates from dynamo action of conductive fluids in the Earth's deep interior [6];
2. An **induced field** caused by magnetic induction in magnetically susceptible earth materials polarized by the main field [7];
3. A field caused by **remanent magnetism** of earth materials [7]; and
4. Other (usually) less significant fields caused by solar, atmospheric [8] and cultural influences

While we can handle the external features (source 4) component (like drift correction in gravity survey: for the solar/atmospheric sources) and divesting from such features or recognizing their transient effects and removing them (for cultural features), the main field is examined from complex models that have been developed and are available. Our intent here is to characterize the global magnetic field (main field) in order to isolate the magnetic field caused by crustal sources (sources 2 and 3).

Spherical harmonic analysis provides the means with which to determine from measurements of a potential field and its gradient on a sphere whether the sources of the field lie within the sphere or outside the sphere. Carl Friederich Gauss in 1838 was the first to describe the geomagnetic field in this way and concluded that the observed field at the Earth's surface originates entirely from within the Earth. However, we know today from satellite observations, space probes and vast accumulation of information from field measurements that a small part of the geomagnetic field originates from outside the Earth.

http://dx.doi.org/10.5772/57163

We consider a magnetic induction vector, $\vec{B}$ at a point on or above the Earth's surface and its potential, V, such that $\vec{B} = -\nabla V$. If we assume a source-free space, V is harmonic and satisfies Laplace's equation:

$$\nabla^2 V = 0 \tag{4}$$

Following [9], if no sources exist outside the sphere, then both V and $\frac{\partial V}{\partial r}$ must vanish for $r \to \infty$ and hence:

$$V^i = a\sum_{n=0}^{\infty}\left(\frac{r}{a}\right)^{n+1}\sum_{m=0}^{n}\left(A_n^{mi}\cos m\varphi + B_n^{mi}\sin m\varphi\right)P_n^m(\theta) : r \geq a \tag{5}$$

On the other hand, if all sources lie outside the sphere, then V and $\frac{\partial V}{\partial r}$ must be finite within the sphere and appropriately,

$$V^e = a\sum_{n=0}^{\infty}\left(\frac{r}{a}\right)^{n}\sum_{m=0}^{n}\left(A_n^{me}\cos m\varphi + B_n^{me}\sin m\varphi\right)P_n^m(\theta) : \; r \geq a \tag{6}$$

Where in both equations (5) and (6), the superscripts, i and e denote internal and external sources respectively, θ is the co-latitude (latitude = 90° - θ), ϕ is longitude, r is the radial distance from the centre of the sphere, a is the radius of the sphere, and $P_n^m(\theta)$ is an associated Legendre polynomial of degree n and order m normalized according to the convention of Schmidt. The magnitude of the normalized Schmidt surface harmonics when squared and averaged over the sphere can be expressed as

$$\frac{1}{4\pi r^2}\int_0^{2\pi}\int_0^{\pi} P_n^m(\theta)\left\{\begin{matrix}\cos m\varphi \\ \sin m\varphi\end{matrix}\right\}P_{n'}^{m'}(\theta)\left\{\begin{matrix}\cos m'\theta \\ \sin m'\varphi\end{matrix}\right\}r^2\sin\theta\, d\theta d\varphi = \begin{cases}0 & n \neq n' \text{ or } m \neq m' \\ \dfrac{1}{2n+1} & n = n' \text{ and } m = m'\end{cases} \tag{7}$$

For example, the normalized surface harmonics for n = 0, m = 0 is 1, for n = 1, m = 0 is cosθ, for n = 1, m = 1 is $\sin\theta\left\{\begin{matrix}\cos \\ \sin\end{matrix}\right\}\varphi$, etc.

Different types of surface harmonics can be deduced from the nature and forms of the normalized term: $P_n^m(\theta)\left\{\begin{matrix}\cos m\varphi \\ \sin m\varphi\end{matrix}\right\}$. If m = 0, the surface harmonic depends on colatitude, θ or latitude (90° – θ) as the longitude component vanishes. This surface harmonic is called the zonal harmonic. If n-m = 0, the surface harmonics depends on longitude and is called the sectoral harmonic (resembles the sectors of an orange). If m > 0 and n-m > 0, the harmonic is termed as tesseral harmonic. These harmonics are useful in characterizing the relative importance of coefficients A_n^m and B_n^m in equations (5) and (6).

If sources exist both inside and outside the sphere, then the potential, V in source-free regions near the surface of the sphere is given by the sum of the equations (5) and (6). Thus it is further

convenient to express the combination of equations (5) and (6) in terms of Gauss' coefficients g_n^m and h_n^m for free-space (where the permeability, $\mu_0 = 1$ c.g.s.). Thus

$$V = a\sum_{n=1}^{\infty}\left(\frac{a}{r}\right)^{n+1}\sum_{m=0}^{n}\left[g_n^m\cos m\varphi + h_n^m\sin m\varphi\right]P_n^m(\theta) \tag{8}$$

It is generally known that n = 1 harmonic from equation (8) gives the first three coefficients (g_1^0, g_1^1 and h_1^1) which have overwhelming dominance. There is no g_0^0 term as this corresponds to the potential of a monopole which must therefore be zero. The first degree harmonic describes the potential of a dipole at the centre of the sphere and therefore the large amplitudes of these coefficients reflect the generally geocentric dipolar character of the main geomagnetic field.

Excluding the n = 1 harmonic from equation (8) eliminates the dipole term from the geomagnetic field and leaving a remainder of the form called the non-dipole part.

At the point of observation, P, T is the magnitude of the total field intensity, and X, Y, Z and H are the north, east, vertical and horizontal components respectively. The quantity, I is the angle T makes with the horizontal (along which H is directed) and is called the dip or inclination, while D, the declination is the angle the horizontal field, H makes with the true or geographic north. Note that H is not the same here as the one expressed in equation (2).

We note that a simple dipole theory predicts that the magnetic inclination, I is related to the geographic latitude, φ as $\tan I = 2\tan\varphi$.

The vector elements of the Earth's magnetic field at a point are $\vec{T}$, $\vec{X}$, $\vec{Y}$, $\vec{Z}$, D, I. Like the reference ellipsoid and theoretical gravity, the mathematical representation of the low-degree parts of the geomagnetic field is determined by international agreement. This mathematical description is called the International Geomagnetic Reference Field (IGRF) and is attributed to the International Association of Geomagnetism and Aeronomy (IAGA) and its umbrella organization, the International Union of Geodesy and Geophysics (IUGG).

The IGRF is essentially a set of Gaussian coefficients, g_n^m and h_n^m that are put forth every 5 years by IAGA for use in a spherical harmonic model. At each of these epoch years, the group considers several proposals and typically adopts a compromise that best fits the data available. The coefficients for a given epoch year are referred to by IGRF and then the year, as in IGRF2000. The model includes both the coefficients for the epoch year and secular variation variables, which track the change of these coefficients in nanotesla per year. These secular variation coefficients are used to extrapolate the Gaussian coefficients to the date in question. Once data become available about the actual magnetic field for a given epoch year, the model is adjusted and becomes the Definitive Geomagnetic Reference Field, or DGRF.

Practically the IGRF consists of Gauss' coefficients through degree and order 10 or slightly above as these terms are believed to represent the larger part of the field of the Earth's core. Subtracting these low-order terms from the measured magnetic fields provides in principle the magnetic field of the crust.

4. Similarities and differences with gravity methods

The gravity and magnetic survey methods exploit the fact that variations in the physical properties of rocks in-situ give rise to variations in some physical quantity which may be measured remotely (on are above the ground). In the case of gravity method, the physical rock property is density and so density variations at all depths within the Earth contribute to the broad spectrum of gravity anomalies. For the magnetic method, the rock property is magnetic susceptibility and/or remanent magnetization; both of which can only exist at temperatures cooler than the Curie point and thus restricting the sources of magnetic anomalies to the uppermost 30 – 40 km of the Earth's interior. In practice, almost all magnetic properties of rocks in bulk reflect the properties and concentrations of oxides of iron and titanium (Fe and Ti): the Fe-Ti-O system, plus one sulphide mineral, pyrrhotite [1]. We also note that the highest density used typically in gravity surveys are about 3.0 g cm^{-3}, and the lowest densities are about 1.0 g cm^{-3}. Thus densities of rocks and soils vary very little from place to place. On the other hand, magnetic susceptibility can vary as much as four to five orders of magnitude from place to place, even within a given rock type.

Magnetic method	Gravity method
Passive and is a potential field bearing all the consequences	Passive and is a potential field bearing all the consequences
Mathematical expression for the force field is that of the inverse square law relation	Mathematical expression for the force field is that of the inverse square law relation
Force between monopoles can either be attractive or repulsive	Force between masses is always attractive
A monopole cannot be isolated. Monopoles always exist in pairs (dipole)	A single point mass can be isolated
A properly reduced field has variation due to variation in induced magnetization of susceptible rocks and remanent magnetization	A properly reduced field has variation due to density variation in rocks
Field changes significantly over time (secular variation).	Field does not change significantly over time.

Table 1. Other similarities and differences between gravity and magnetic methods

5. The magnetic properties of rocks

Geologic interpretation of magnetic data requires the knowledge of the magnetic properties of rocks in terms of magnetic susceptibility and remanent magnetization. Factors that influence rock magnetic properties for various rock types have been summarized appropriately [10], [1], [11], [12]. The rocks of the Earth's crust are in general only weakly magnetic but can exhibit both induced and remanent magnetizations. Magnetic properties of rocks can only exist at

temperatures below the Curie point. The Curie temperature is found to vary within rocks but is often in the range 550°C to 600°C [13]. Modern research indicates that this temperature is probably reached by the normal geothermal gradient at depths between 30 and 40 km in the Earth and this so-called 'Curie point isotherm' may occur much closer to the Earth's surface in areas of high heat flow.

Indeed rock magnetism is a subject of considerable complexity. Clearly, all crustal rocks find themselves situated within the geomagnetic field described in section 3. These crustal rocks are therefore likely to display induced magnetization given by equation (3), where the magnitude of magnetization, J_i is proportional to the strength of the Earth's field, T. The magnetic susceptibility, k is actually the magnetic volume susceptibility that is encountered in exploration rather than mass or molar susceptibilities.

Apart from the induced magnetization, many rocks also show a natural remanent magnetization (NRM) that would remain even if the present-day geomagnetic field ceases to exist. The simplest way in which NRM can be acquired is through the process of cooling of rocks in molten state. As the rocks cool past the Curie point (or blocking temperature) a remanent magnetization in the direction of the prevailing geomagnetic field will be acquired. The magnitude and direction of the remanent magnetization can remain unchanged regardless of any subsequent changes in the ambient field.

6. Measurement procedures of magnetic field

Measurements can be made of the Earth's total magnetic field or of components of the field in various directions. The oldest magnetic prospecting instrument is the magnetic compass, which measures the field direction. Other instruments include magnetic balances and fluxgate magnetometers.

The most used instruments in modern magnetic surveys are the proton-precession or optical-pumping magnetometers and these are appreciably more accurate and all of these instruments give absolute values of field. The proton magnetometer measures a radio-frequency voltage induced in a coil by the reorientation (precession) of magnetically polarized protons in a container of ordinary water or paraffin. Its measurement sensitivity is about 1 nT. The optical-pumping magnetometer makes use of the principles of nuclear resonance and cesium or rubidium vapour. It can detect minute magnetic fluctuations by measuring the effects of light-induced (optically pumped) transitions between atomic energy levels that are dependent on the strength of the prevailing magnetic field. The sensitivity of the optical absorption magnetometer is about 0.01 nT and on this premise may be preferred to proton precession magnetometer in air-borne surveys.

Airborne magnetic surveys or aeromagnetic surveys are usually made with magnetometers carried by aircraft flying in parallel lines spaced 2 - 4 km apart at an elevation of about 500 m when exploring for petroleum deposits and in lines 0.5 - 1.0 km apart roughly 200 m or less above the ground when searching for mineral concentrations. Ship-borne magnetic surveys

http://dx.doi.org/10.5772/57163

or marine magnetic surveys can also be completed over water by towing a magnetometer behind a ship.

Ground surveys are conducted to follow up magnetic anomaly discoveries made from the air. Such surveys may involve stations spaced from 50 m apart. Survey may be along profiles or gridded network or may be in random pattern. Magnetometers also are towed by research vessels or mounted on the researcher on foot. In some cases, two or more magnetometers displaced a few metres from each other are used in a gradiometer arrangement; differences between their readings indicate the magnetic field gradient. A ground monitor is usually used to measure the natural fluctuations of the Earth's field over time so that corrections similar to drift correction in gravity can be made. Alternatively, like gravity observations where the temporal variation in field values were accounted for by reoccupying a base station and using the variation in this reading to account for instrument drift and temporal variations of the field, we could also use the same strategy in acquiring magnetic observations. The alternative is not the best as field variation in magnetic may be highly erratic and magnetometers which are electronic instruments do not drift. With these points in mind most investigators conduct magnetic surveys using two magnetometers. One is used to monitor temporal variations of the magnetic field continuously at a chosen "base station", and the other is used to collect observations related to the survey proper.

Surveying is generally suspended during periods of large magnetic fluctuation (magnetic storms).

7. Magnetic anomalies

Magnetic effects result primarily from the magnetization induced in susceptible rocks by the Earth's magnetic field. Most sedimentary rocks have very low susceptibility and thus are nearly transparent to magnetism. Accordingly, in petroleum exploration magnetics are used negatively: magnetic anomalies indicate the absence of explorable sedimentary rocks. Magnetics are used for mapping features in igneous and metamorphic rocks, possibly faults, dikes, or other features that are associated with mineral concentrations. Data are usually displayed in the form of a contour map of the magnetic field, but interpretation is often made on profiles.

The first stage in any ground magnetic survey is to check the magnetometers and the operators. Operators can be potent sources of magnetic noise. Errors can also occur when the sensor of the magnetometer is carried on a short pole or on a back rack. Compasses, pocket knives, metal keys, geological hammers, and cultural articles with metal blend (belt, shoes, bungles, etc) are all detectable at distances below about a metre and therefore the use of high-sensitivity magnetometers requires that operators divest themselves of all metallic objects. Attempts must be made to follow the operation manual provided along with a magnetometer!

Diurnal corrections are essential in most field work, unless only gradient data are to be used. If only a single magnetometer is available, diurnal corrections have to rely on repeated visits to a base, ideally at intervals of less than an hour. A more robust diurnal curve can be con-

structed if a second fixed magnetometer is used to obtain readings at 3 to 5 minute intervals. The second magnetometer need not be the same type as that being used in the field. Thus a proton magnetometer can provide adequate diurnal control for surveys conducted with cesium vapour magnetometer and vice versa. Note that base should be remote from magnetic interferences and must be describable for future use.

In aeromagnetic surveys, great pains must be taken to eliminate spurious magnetic signals that may be expected to arise from the aircraft itself. Airframes of modern aircraft are primarily constructed from aluminum alloys which are non-magnetic and so the potential magnetic sources are the aircraft engines. Thus magnetometer sensors must be mounted far away from these engines.

Aeromagnetic data usually obtained have gone through on-board processing such as magnetic compensation, checking/editing, diurnal removal, tie line and micro leveling. For example, the basis of magnetic compensation is the reduction of motion-induced noise on the selected magnetic elements. These can be from individual sensors or various gradient configurations. The motion noise comes from the complex three-dimensional magnetic signature of the airframe as it changes attitude with respect to the magnetic field vector. The noise comes from permanent, induced and eddy effects of the airframe plus additional heading effects of the individual sensors. Thus the magnetic interference in a geophysical aircraft environment comes from several sources which must be noted and compensated for.

On-board data checking and editing involves the removal of spurious noise and spikes from the data. Such noise can be caused by cultural influences such as power lines, metallic structures, radio transmissions, fences and various other factors. Diurnal removal corrects for temporal variation of the earth's main field. This is achieved by subtracting the time-synchronized signal, recorded at a stationary base magnetometer, from survey data. Alternatively, points of intersection of tie lines with traverse/profile lines can form loop networks which can be used to correct for the diurnal variation similar to drift correction in gravity survey.

Tie leveling utilizes the additional data recorded on tie lines to further adjust the data by consideration of the observation that, after the above corrections are made, data recorded at intersections (crossover points) of traverse and tie lines should be equal. Several techniques exist for making these adjustments and [14] gives a detailed of the commonly used techniques. The most significant cause of these errors is usually inadequate diurnal removal. Micro-leveling, on the other hand, is used to remove any errors remaining after the above adjustments are applied. These are usually very subtle errors caused by variations in terrain clearance or elevated diurnal activity. Such errors manifest themselves in the data as anomalies elongate in the traverse line direction. Accordingly they can be successfully removed with directional spatial filtering techniques [15].

When all the above considerations to raw magnetic data have been recognized and attended to, the IGRF correction (main field effect) is now carried out to give the 'magnetic anomaly' defined as the departure of the observed field from the global model.

http://dx.doi.org/10.5772/57163

8. Potential fields and models

8.1. Potential field in source free space

The potential field, φ (x, y, z) in free space, i.e. without any sources satisfies the Laplace equation $\nabla^2\varphi = 0$ or when sources are present the potential satisfies the so-called Poisson equation, $\nabla^2\varphi = -\rho(x, y, z)$, where ϱ (x, y, z) stands for density or magnetization depending upon whether φ stands for gravity or magnetic potential. Laplace's equation has certain very useful properties particularly in source-free space such as the atmosphere where most measurements are made. Some of these properties are (1) given the potential field over any plane, we can compute the field at almost all points in the space by analytical continuation; (2) the points where the field cannot be computed are the so-called singular points. A closed surface enclosing all such singular points also encloses the sources which give rise to the potential field. These properties of the potential field are best brought out in the Fourier domain.

The Fourier transform in one-dimension can be found in most text books of applied mathematics. The Fourier transform in two or three dimensions possess additional properties worth noting [16]. The two-dimensional Fourier transform is given by: $\Phi(u, v) = \iint_{-\infty}^{+\infty} \varphi(x, y) e^{-i(ux+vy)} dxdy$ and its inverse is given by $\varphi(x, y) = \frac{1}{4\pi^2} \iint_{-\infty}^{+\infty} \Phi(u, v) e^{i(ux+vy)} dudv$

Where u and v are spatial frequency numbers in the x- and y-directions respectively ($u = 2\pi/L_x$ and $v = 2\pi/L_y$), with L_x and L_y as length dimensions in the x- and y-directions respectively. It is important to note that φ (x, y) and Φ (u, v) are simply different ways of looking at the same phenomenon. The Fourier transform maps a function from one domain (space or time) into another domain (wave number or frequency). For details, [17] can be consulted.

Magnetic potential field is caused by the variation in magnetization in the Earth's crust. This potential field is observed over a plane close to the surface of the Earth. If the magnetization variations are properly modeled consistent with other geological information, it is possible to fit the model to the observed potential field. Note that the magnetic field induction usually observed is the derivative of this potential. The model parameters (body shape factors, susceptibility values, burial depth, and magnetization direction) are then observable. These models may be (1) excess magnetization confined to a well-defined geometrical object, (2) geological entity such as basins (sedimentary or metamorphic with intrusive bodies). Sedimentary basins are of great interest on account of their hydrocarbon potential and since these rocks are generally non-magnetic, the observed magnetic field is probably entirely due to the basement on which sediments are resting and (3) with available resources and technology (as in airborne magnetic surveys) large areas can be covered in a survey and so permitting maps that cover several geological provinces or basins and therefore allow inter basin studies such as delineating of extensive shallow and deep features as faults, basin boundaries, etc. to be extracted.

We shall briefly outline a few examples of the rigors that an interpreter goes through to synthesize information from these potential fields.

8.2. Dipole field

We consider two monopoles of opposite sign: one at the origin of the 3-coordinate system and the other positioned below such that their common axis is along the z-axis, with -Δz as the separation between the monopoles (Fig. 2)

The potential at P, V (P) due to both monopoles is the sum of the potentials caused by each monopole. This is given generally for monopoles that are not aligned along any particular axis as [18]:

$$V(P) = -C_m \vec{m}.\vec{\nabla}_P\left(\frac{1}{r}\right) \tag{9}$$

Where $\vec{m}$ is the dipole moment ($\vec{m} = q\vec{ds}$ with q as the pole strength and $\vec{ds}$ is the displacement from monopole 1 to monopole 2.), C_m is the Coulomb's law constant ($C_m = \mu_0/4\pi$: μ_0 is the permeability of free space) and ∇_P is the derivative vector operator towards point P.

According to Helmholtz theorem, the magnetic field, $\vec{B}$ can be derived from this potential, V (P) such that $\vec{B} = -\vec{\nabla}_P V(P)$. Using this on equation (9) yields

$$\vec{B} = C_m \frac{m}{r^3}[3(\hat{m}.\hat{r})\hat{r} - \hat{m}], \quad r \neq 0 \tag{10}$$

Where m is the magnitude of the dipole moment while $\hat{r}$ and $\hat{m}$ are unit vectors in the increasing r and m directions respectively. Thus equation (10) shows that the magnitude of $\vec{B}$ is proportional to the dipole moment and inversely proportional to the cube of the distance to the pole.

Equation (10) can also be expressed in cylindrical coordinates as [8]:

$$\vec{B} = C_m \frac{m}{r^3}(3\cos\theta\hat{r} - \hat{m}) \tag{11}$$

Where θ is now the angle between $\hat{m}$ and $\hat{r}$ so that with $\vec{B} = -\vec{\nabla}_P V$, we can compute the components of the field in the directions of r and θ, respectively as $\vec{B}_r$ and $\vec{B}_\theta$ expressed as

$\vec{B}_r = -\hat{r}\frac{\partial V}{\partial r} = 2C_m\frac{m\cos\theta}{r^3}$, $\vec{B}_\theta = -\hat{\theta}\frac{1}{r}\frac{\partial V}{\partial \theta} = C_m\frac{m\sin\theta}{r^3}$ and so the magnitude of $\vec{B}$ is expressed as

$$|\vec{B}| = \sqrt{|\vec{B}_r|^2 + |\vec{B}_\theta|^2} = C_m\frac{m}{r^3}(3\cos^2\theta + 1)^{1/2} \tag{12}$$

Equation (12) shows that the magnitude $|\vec{B}|$ of the dipole field along any direction extending from the dipole decreases at a rate inversely proportional to the cube of the distance to the dipole. The magnitude of $\vec{B}$ also depends on θ.

Many magnetic bodies exist that are dipolar in nature to a first approximation. For example, the entire field of the Earth appears nearly dipolar from the perspective of other planets. It is also known that in aeromagnetic survey, the inhomogeneity of a massive pluton at the survey height appears to be a dipole source.

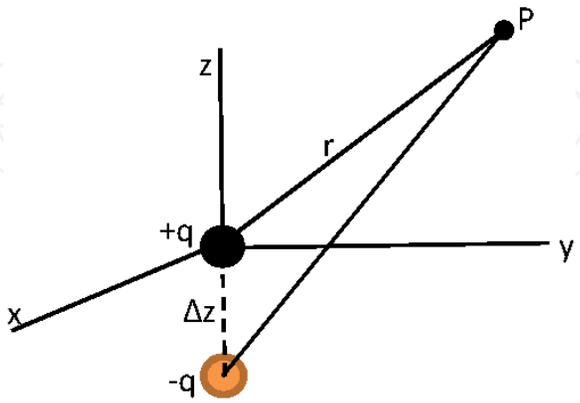

Figure 2. Two monopoles of opposite sign with the monopole of positive sign at the origin and other situated at z = Δz

8.3. Three-dimensional distribution of magnetization

We can consider a small element of magnetic material of volume, dv and magnetization, $\vec{M}$ (Fig. 3) to act like a single dipole such that $\vec{M}\,dv = \vec{m}$. Then the potential at some point, P outside the body is given as in equation (9) to be

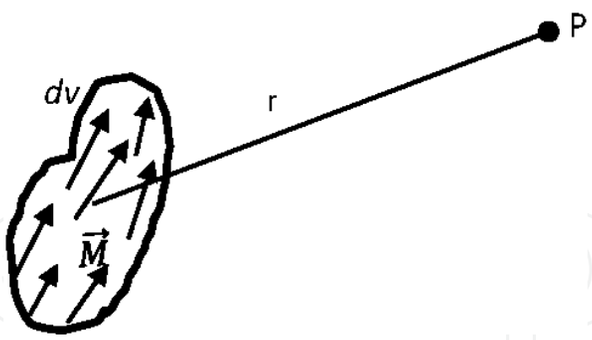

Figure 3. A 3-D magnetic body of volume dv and uniform magnetization $\vec{M}$

$$V(P) = -C_m \vec{M} . \vec{\nabla}_P \left(\frac{1}{r}\right) dv \tag{13}$$

Where r again is the distance from P to the dipole. In general, magnetization, $\vec{M}$ is a function of position where both direction and magnitude can vary from point to point, i.e. $\vec{M} = \vec{M}(Q)$, where Q is the position of the volume element, dv. Integrating equation (13) over all elemental volumes provides the potential of a distribution of magnetization as

$$V(P)=C_m\int\vec{M}(Q).\vec{\nabla}_Q\left(\frac{1}{r}\right)dv \tag{14}$$

The magnetic induction, $\vec{B}$ at P is then given by

$$\vec{B}(P)=-\vec{\nabla}_P V(P)=-C_m\vec{\nabla}_P\int\vec{M}(Q).\vec{\nabla}_Q\left(\frac{1}{r}\right)dv \tag{15}$$

The subscripts in the gradient operator from P to Q are now $\vec{\nabla}_P$ and $\vec{\nabla}_Q$ when the operator is inside the volume integral showing that the gradient is taken with respect to the source coordinates rather than with respect to the observation point.

For a two-dimensional source, we may start with a body of finite length 2a and so the volume integral in equation (15) is replaced with surface integral over the cross sectional area, dS of the body and a line integral along its length (the z-axis) as:

$$\begin{aligned} V(P)&=C_m\int\mathbf{M}(Q).\nabla_Q\left(\frac{1}{r}\right)dv=C_m\int\mathbf{M}(Q).\left(\int_{-a}^{a}\nabla_Q\left(\frac{1}{r}\right)dz\right)dS \quad \text{(a)}\\ V(P)&=2C_m\int\frac{\mathbf{M}(Q).\hat{r}}{r}dS \quad \text{(b)}\end{aligned} \tag{16}$$

Where S is the cross sectional area of the body. As $a\rightarrow\infty$ (a 2-D case), the integral approaches a potential of infinite line of dipoles of unit magnitude. Hence (16b).

The magnetic field induction, $\vec{B}(P)$ can be obtained from equation (16b) as:

$$\vec{B}(P)=-\vec{\nabla}V(P)=2C_m\int\frac{M(Q)}{r^2}[2(\hat{M}.\hat{r})\hat{r}-\hat{M}]dS \tag{17}$$

Note also that $\hat{r}$ is the normal to the long axis of the cylinder and r is a perpendicular distance.

8.4. Poisson relation

We had noted in section one, and by implication, that the mutual force, F between a particle of mass m_1 centred at point Q (x', y', z') and a particle of mass, m_2 at P (x, y, z) is given by

$$F=G\frac{m_1m_2}{r^2} \tag{18}$$

Where $r=[(x-x')^2+(y-y')^2+(z-z')^2]^{1/2}$. If we let m_2 be a test particle with unit magnitude, then the gravitational attraction, $\vec{g}(P)$ produced by m_1 at the location P of m_2 (the test particle) is

$$\vec{g}(P)=-G\frac{m_1}{r}\hat{r} \tag{19}$$

Where $\hat{r}$ is a unit vector directed from m_1 to the observation point, P and expressed as $\hat{r}=\frac{1}{r}[(x-x')\hat{i}+(y-y')\hat{j}+(z-z')\hat{k}]$ and the minus sign in equation (19) indicates that as r increases $\vec{g}(P)$ decreases in absolute value.

If a potential exists, then the gravitational attraction (also known as the gravitational acceleration), $\vec{g}(P)$ can be derived from this potential. Let this potential be U. Then at P, U = U (P), such that

$$\vec{g}(P)=-\vec{\nabla}U(P) \tag{20}$$

Where here, U (P) can be expressed as

$$U(P)=G\frac{m_1}{r^2} \tag{21}$$

Where the gravitational potential is defined as the work done by the field on the test particle.

Equations (19) and (12) show that the magnetic scalar potential of an element of magnetic material and the gravitational attraction of mass are identical. Starting from equation (13), and considering a body with uniform magnetization, $\vec{M}$ and uniform density, ϱ, the magnetic scalar potential at a point, P is

$$V(P)=-C_m\int\vec{M}.\vec{\nabla}_P\left(\frac{1}{r}\right)dv=-C_m\vec{M}.\vec{\nabla}_P\int\frac{1}{r}dv \tag{22}$$

The gravitational potential (equation (22)) is written as

$U(P)=G\int\frac{\rho}{r}dv=G\rho\int\frac{1}{r}dv$, so that $\int\frac{1}{r}dv=\frac{U(P)}{G\rho}$ and substituting this in equation (21) gives

$$V(P)=-\frac{C_m}{G\rho}\vec{M}.\vec{\nabla}_P U(P)=-\frac{C_mM}{G\rho}g_m \tag{23}$$

Where g_m is the component of gravity in the direction of magnetization and M is the magnitude of the magnetization.

Equation (23) is the so-called Poisson's relation and can be stated as follows: if the boundaries of a gravitational and magnetic source are the same and its magnetization and density distribution being uniform, then the magnetic potential is proportional to the component of gravitational attraction in the direction of magnetization, i.e. $V(P)\propto\vec{M}.\vec{g}(P)$.

Poisson relation can be used to transform a magnetic anomaly into pseudo-gravity, the gravity anomaly that would be observed if the magnetization were replaced by a density distribution of exact proportions [19]. Pseudo-gravity transformation is a good aid in interpretation of magnetic data. In addition, Poisson's relation can be used to derive expressions for the magnetic induction of simple bodies when the expression for gravitation attraction is known.

8.5. Magnetic field over simple geometrical bodies

The form of magnetic anomaly from a given body is complex and generally depends on the following factors:

i. The geometry of the body

ii. The direction of the Earth's field at a location of the body

iii. The direction of polarization of the rocks forming the body

iv. The orientation of the body with respect to the direction of the Earth's field

v. The orientation of the line of observation with respect to the axis of the body.

Thus the computations of models to account for magnetic anomalies are much more complex than those for gravity anomalies. As earlier stated, when the gravity expressions for simple geometrical bodies are given, we can use the Poisson's relation to find the magnetic expressions over these models [18]. Table 2 is a summary of few of such computations.

Shape of Body	Gravity potential, U	Magnetic potential, V	Magnetic field, $\vec{B} = \vec{\nabla} V$
Sphere of radius, *a*	$\frac{4}{3}\pi a^3 \frac{G\rho}{r}$	$C_m \frac{\vec{m}.\hat{r}}{r^2}$	$C_m \frac{m}{r^3}[3(\hat{m}.\hat{r})\hat{r} - \hat{m}]$
Horizontal cylinder of infinite length of cross sectional radius, r	$2\pi a^2 \rho G \log\left(\frac{1}{r}\right)$	$2C_m \pi a^2 \frac{\vec{M}.\hat{r}}{r}$	$\frac{2C_m m'}{r^2}[2(\hat{m}'.\hat{r})\hat{r} - \hat{m}']$
Horizontal slab of thickness, t	$2\pi\rho Gtz$	$-2\pi C_m Mt$	Zero

Table 2. Gravity and magnetic potentials caused by simple sources, along with magnetic induction for bodies of uniform density, ρ and magnetization, $\vec{M}$ observed at some point, P (x, y, z) away from the centre of the body (other symbols are defined as in section 8.2)

9. Magnetic data processing and interpretation

The total-field magnetic anomaly of section 7 which was obtained by subtracting the magnitude of a suitable regional field (the IGRF or DGRF model for the survey date) from the total-field measurement is referred to as the crustal field. As earlier stated, this field is a vector sum of the remanent and the induced fields of the magnetically susceptible rocks of the crust down to the bottom of the Curie depth. The induced field component is usually in the same direction as the ambient field during the survey period.

Magnetic data processing includes everything done to the data between acquisition and the creation of an interpretable profile map or digital data set. Apart from the effect earlier discussed which are ignored or avoided, rather than corrected for, the correction required for ground magnetic data are insignificant especially when compared to gravity. The influence of

topography (terrain) on ground magnetics on the other hand can be significant. Magnetic terrain effects can severely mask the signatures of underlying sources as demonstrated by [20]. Many workers have attempted to remove or minimize magnetic terrain effects by using some form of filtering as summarized in [21].

Interpretation of magnetic anomalies has to do with (a) studying the given magnetic map, profile or digital data to have a picture of the probable subsurface causes (qualitative interpretation), (b) separating the effect of individual features on the basis of available geophysical and geological data (further separation of broad-based or long-wavelength anomalies) and (c) estimating the likely parameters of the bodies of interest from the corresponding 'residual' or anomalies (quantitative interpretation).

The last two categories of interpretation procedures can be further broken into three parts. Each part has the goal of illuminating the spatial distribution of magnetic sources, but they approach the goal with quite different logical processes.

1. **Forward method:** an initial model for the source body is constructed based on geologic and geophysical intuition. The initial model anomaly is calculated and compared with the observed anomaly; and model parameters are adjusted in order to improve the fit between the two anomalies until the calculated and observed anomalies are deemed sufficiently alike. Forward method is source modeling in which magnetic anomalies were interpreted using characteristics curves [22] calculated from simple models (before the use of electronic computers) or using computer algorithms. Such schemes include 2-D magnetic models [23] and many workers that followed), 3-D magnetic models [24] and many other improvements that followed), Fourier-based models [25] and other improvements that followed) and voxel-based models [26] and others that followed).

2. **Inverse method:** one or more body parameters are calculated automatically and directly from the observed anomaly through some plausible assumptions of the form of the source body. Under this category, we have depth-to-source estimation techniques such as Werner deconvolution [27] and other workers that followed), frequency-domain techniques [28] and others that followed), Naudy matched filter based method [29] and others that followed), analytic signal method [30], [31] and others that followed), Euler deconvolution [32] and others that followed), source parameter imaging [33] and others that followed) and statistical methods [34] and others that followed). Physical property mapping under the inverse method include terracing [35] and susceptibility mapping [36] and others that followed). Other inversion techniques have to do with automated numerical procedures which construct models of subsurface geology from magnetic data and any prior information [37], [38], [39], [40], [41] among many others).

3. **Data enhancement and display:** model parameters are not calculated, but the anomaly is processed in some way in order to enhance certain characteristics of the source bodies, thereby facilitating the overall interpretation. This category involves all filter-based analyses such as reduction to pole (RTP) and pseudogravity [19] and others that followed), upward/downward continuation [42] and others that followed), derivative filters [43] and many others), matched filtering [44] and others that followed) and wavelet transforms

[45] and others that followed). Some of the enhancement techniques are artificial illumination [46], automatic gain control [47] and textural filtering [48]. Data displays can be in form of stacked profiles, contour maps, images and bipole plots.

In summary, any geophysical survey has two domains or spaces of interest: data space (data collected from the field) and model space (earth models) that account for the data space. The task is to establish a link between a data space and a model space (Fig.4).

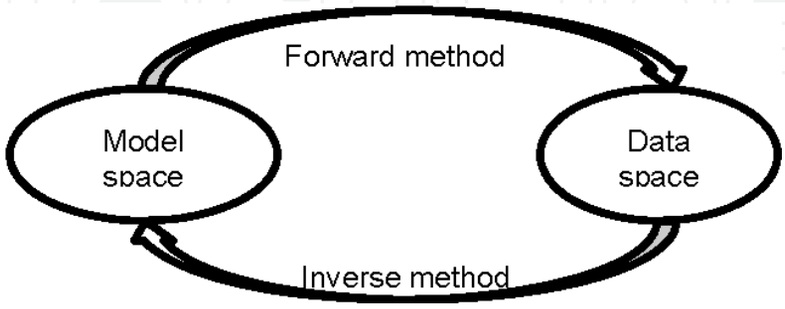

Figure 4. Connecting link between data space and model space in forward and inverse method

The task of retrieving complete information about model parameters from a complete and precise set of data is inversion. Thus if we have a set of data collected from the field, we try to say about the earth model with those finite data set. How many different ways can one try to travel within a data space and a model space? What difficulties are encountered? How many different ways can one try to overcome those difficulties? How much information can one really gather and what are their limitations? What precautions should be taken as one moves from one space to another? Inverse theory seems to address these questions. Inverse method is a direct method in which source parameters are determined in a direct way from field (e.g. magnetic field) measurements.

Forward method on the other hand entails starting from model space (Fig. 4) by guessing initial model parameters and then calculating the model anomaly (in data space). The model anomaly is compared with observed (data) anomaly. If the match between the two is acceptable, the process stops, otherwise model parameters are adjusted and the process repeated. Forward method is an indirect method.

Various formulae exist for computing magnetic field of regular shapes such as the ones given in Table 2.

Analysis of magnetic data and their various enhancements via a suite of qualitative and quantitative methods as outlined above results in an interpretation of the subsurface geology. Qualitative interpretation relies on the spatial patterns that an interpreter can recognize in the data. Faults, dykes, lineaments and folds are usually identified. Intrusive bodies are often recognized by virtue of the shape and amplitude of their anomalies and so on. For example, detection of a fault in a magnetic map is an important exercise in mineral prospecting. Usually faults and related fractures serve as major channel-ways for the upward migration of ore-bearing fluids. Fault zones containing altered magnetic minerals can be detected from series

of closed lows on contour maps, by inflections or by lows on magnetic profiles or by displaced magnetic marker horizons.

Quantitative interpretation on the other hand is meant to compliment the qualitative method and seeks to provide useful estimates of the geometry, depth and magnetization of the magnetic sources. Broadly categorized as curve matching, forward modeling or inversion, quantitative techniques rely on the notion that simple geometric bodies, whose magnetic anomaly can be theoretically calculated, can adequately approximate magnetically more complex bodies. Geometric bodies such as ellipsoids, plates, rectangular prisms, polygonal prisms and thin sheets can all be calculated. Complex bodies can be built by superposing the effects of several simple bodies. Faults are often modeled using thin sheet model.

Like most other geophysical methods, magnetics is ambiguous to the extent that there are an infinite number of models that have the same magnetic anomaly. Acceptable models should be tested for geological plausibility.

10. Case study: Aeromagnetic field over the upper Benue trough, Nigeria

10.1. Geological framework

The Upper Benue Trough, Nigeria (UBT) is the northern end of the nearly 1000 – km NE-SW trending sediment-filled Benue Trough, Nigeria (Fig. 5). Apart from the adjacent Niger Delta area and the offshore region where oil/gas exploration and production are taking place, the Benue Trough as an inland basin lacks the same full attention of the oil/gas companies. However, with the upbeat in the exploration efforts of the national government towards the search for hydrocarbon prospects of this inland basin, particularly in the light of new oil discoveries in the nearby genetically related basins, attention is directed at the structural setting of this basin.

The Benue Trough as a NE-SW trending sedimentary basin has a Y – shaped northern end (a near E – W trending branch of the Yola – Garoua and north-trending branch of Gongola – Muri) (Fig. 5). The Benue Trough is filled with sediments that range from Late Aptian to Palaeocene in age and whose thickness could reach up to 6000 m at places. The environments of deposition also varied over time such that the sediments vary from continental lacustrine/fluviatile sediments at the bottom through various marine transgressive and regressive beds, to immature reddish continental sands at the top.

For the past 50 years, the published works on the geology of the Benue Trough have substantially increased. The most important regional geological work on the Benue Trough by [49] was a basis for subsequent geological interpretations. [49] interpreted the Benue Trough origin in terms of rift faulting and the folding of the Cretaceous age associated with the basement flexuring. The first geophysical contribution of [50] on the Benue Trough remains to date the unique published reference. These authors have proposed the same rift origin considering that the main boundary rift faults are concealed by the Cretaceous sediments. They observed the existence below the Benue Trough axis, of a central positive gravity anomaly interpreted as a

basement high. Field evidence indicates that a set of deep-seated faults is superimposed on the axial high and controlled the tectonic evolution of the trough.

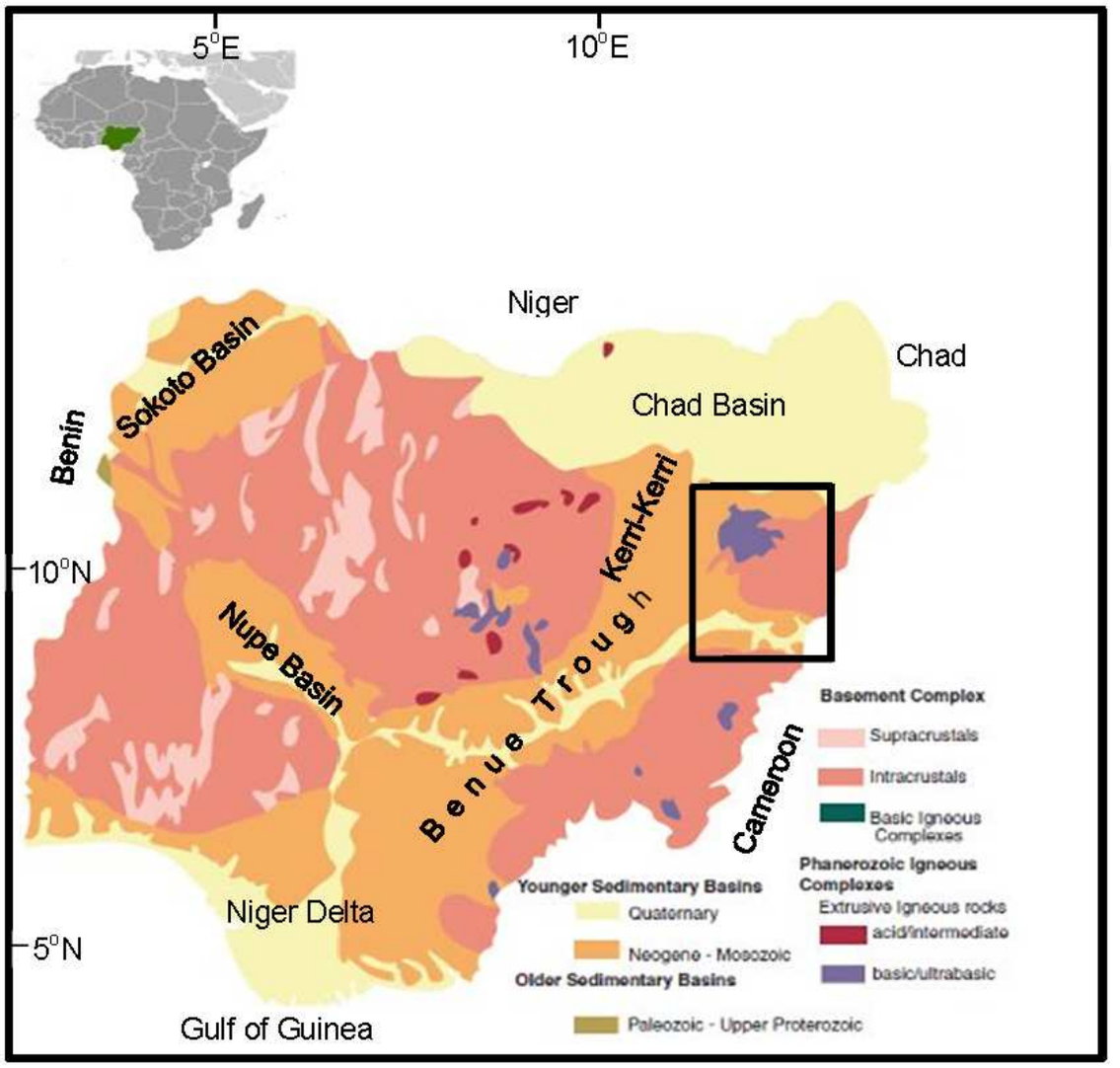

Figure 5. Top is map of Africa showing Nigeria. Below is a simplified geological map of Nigeria (modified from http://nigeriaminers, org). The inset rectangle is the Upper Benue Trough, Nigeria

The rift origin of the Benue Trough supported by numerous authors was interpreted in the plate tectonics concept and from the 1970s several models were proposed to explain the origin of the Benue Trough. For example, seen as a direct consequence of the Atlantic Ocean opening, the Benue Trough was considered to be the third arm of a triple junction located beneath the centre of the present Niger Delta [51] and proposed a Ridge-Ridge-Ridge (RRR) triple junction. This hypothesis has been widely discussed and replaced in the general framework of African Rift System.

The Benue Trough is subdivided into 3 units on the basis of stratigraphic and tectonic considerations. The southern ensemble is called the Lower Benue Trough (LBT) and includes two

main units: the Abakaliki Uplift or Anticlinorium and the Anambra Basin. The Abakaliki Anticlinorium (AA) is formed by tightly folded Cretaceous sediments intruded by numerous magmatic rocks. From the Niger Delta, AA extends for about 250 km to the Gboko – Ogoja area in a N50E direction. To the north of AA is a vast synclinorial structure called the Anambra Basin and trends in a N30E direction. This basin comprises a thick undeformed Cretaceous series. On the northern margin of the Anambra Basin, is the Nupe or Middle Niger Basin which stretches along a NW-SE direction. To the south, AA is flanked by the Afikpo Syncline and by a narrow strip of thin, undeformed sediments resting on the Basement Complex (the Mamfe Basin) and to the northwestern border is the Oban Massif. South of the Oban Massif is the Calabar Flank, which belongs to the coastal basins of the Gulf of Guinea.

The Upper Benue Trough (UBT) which is the northern ensemble is the most complex part (Fig. 5). It is characterized by cover tectonics and can be further subdivided into several smaller units. The Gongola – Muri and Yola – Garoua branches are digitations of the Benue Trough and present a similar tectonic style. The Gongola - Muri rift disappears beneath the Tertiary sediments of the Chad Basin and so the margins of this rift are geologically the most difficult to established. The Yola – Garoua rift to some extent is the least known of the West African Rift and strikes E-W into Cameroon. On the western margin of the UBT is the flat-lying Paleocene Kerri Kerri basin resting unconformably upon the folded Cretaceous. The development of the Kerri Kerri basin is said to be controlled by a set of faults between it and the Basement Complex of the Jos Plateau [52]. The basin formation and its tectonic activity seem to be a response of the general uplift of the UBT due to late Cretaceous folding.

The UBT is contiguous with the Nigerian sector of the Chad Basin which extends northwards into the Termit Basin of Chad and Niger and southwestwards into Cameroon and southern Chad as Bongor, Doba, Doseo and Salamat basins. This rift system is closely linked with oil-rich Muglad Basin of Sudan.

10.2. Aeromagnetic field

Magnetic data over Nigeria have been largely collected above the ground surface in form of systematic surveys on behalf of the national government. These airborne surveys were carried out principally by a consultant, namely: **Fugro Airborne Surveys,** on behalf of the Nigerian Geological Survey Agency (NGSA) between 2003 and 2009. The main aim of these surveys has been to assist in mineral and groundwater development through improved geological mapping. Flight line direction is nearly NW-SE and tie line direction is NE – SW. The flight height average is 100 m; profile line spacing is 500 m with tie line spacing of 2 km. Figure 6 shows one of the aircrafts of Fugro Airborne Surveys in flight.

The total field aeromagnetic field intensity for the UBT comprises 16 half-degree grids acquired from NGSA and is used for the purpose of the present study. These are 131_BAJOGA, 132_GULANI, 133_BIU, 134_CHIBUK; 152_GOMBE, 153_WUYO, 154_SHANI, 155_GARKIDA; 173_KALTUNGO, 174_GUYOK, 175_SHELLEN, 176_ZUMO; 194_LAU, 195_DONG, 196_NUMAN and 197_GIREI total magnetic intensity (TMI) grids.

Figure 6. Fugro Airborne Surveys photo showing a magnetometer in a 'stinger' behind the fixed-wing aircraft.

The aeromagnetic data obtained have gone through on-board processing such as magnetic compensation, checking/editing, diurnal removal, tie line and micro leveling.

The composite total field aeromagnetic data for the UBT are displayed in image (Fig. 7). The advantage of images is that they are capable of showing extremely subtle features not apparent in other forms of presentations (such as contour maps). They can also be quickly manipulated in digital form, thereby providing an ideal basis for on-screen GIS-based applications.

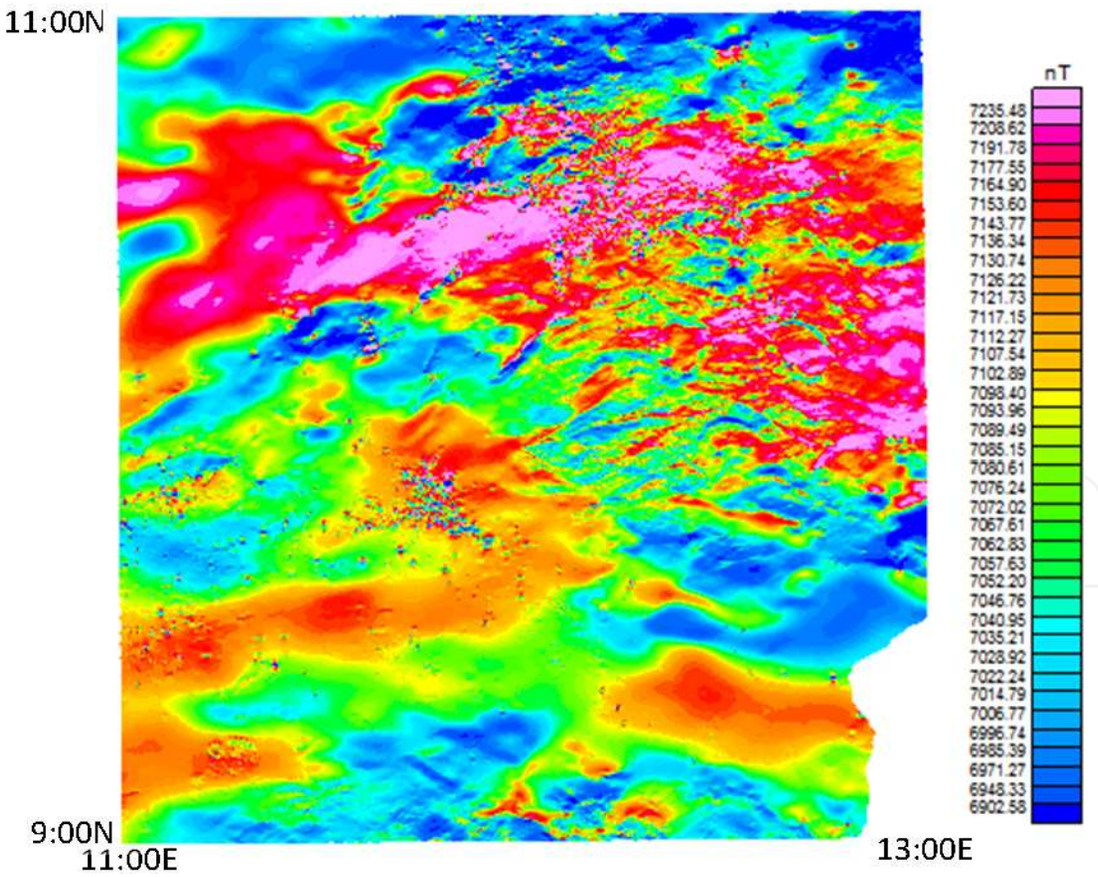

Figure 7. The total-field aeromagnetic intensity over UBT. A base value of 26, 000 nT should be added to map value for the total-field

http://dx.doi.org/10.5772/57163

We have further treated the composite total field aeromagnetic data (Fig. 7) for the UBT for the main field effect through the removal of the Definitive Geomagnetic Reference Field (DGRF – 2005) (Fig. 8) resulting in total magnetic field intensity anomaly (Fig. 9). This anomaly field has polarity signs that shows the impact of low geomagnetic inclination values for the study area and also reflects (1) the **induced field** caused by magnetic induction in magnetically susceptible earth materials polarized by the main field and (2) the field caused by **remanent magnetism** of earth materials. We call these two fields, the crustal field and have used the appropriate software (Geosoft Oasis Montaj version 8.0) for image processing and/or display of both the raw data (Fig. 7) and the anomaly data (Fig. 9). We have noted that a NW-SE mega feature dominated the middle of the study area. This linear feature, which is interrupted somehow towards the NW section of the map area, is believed to be central in the structural configuration and set-up of this Benue Trough subarea.

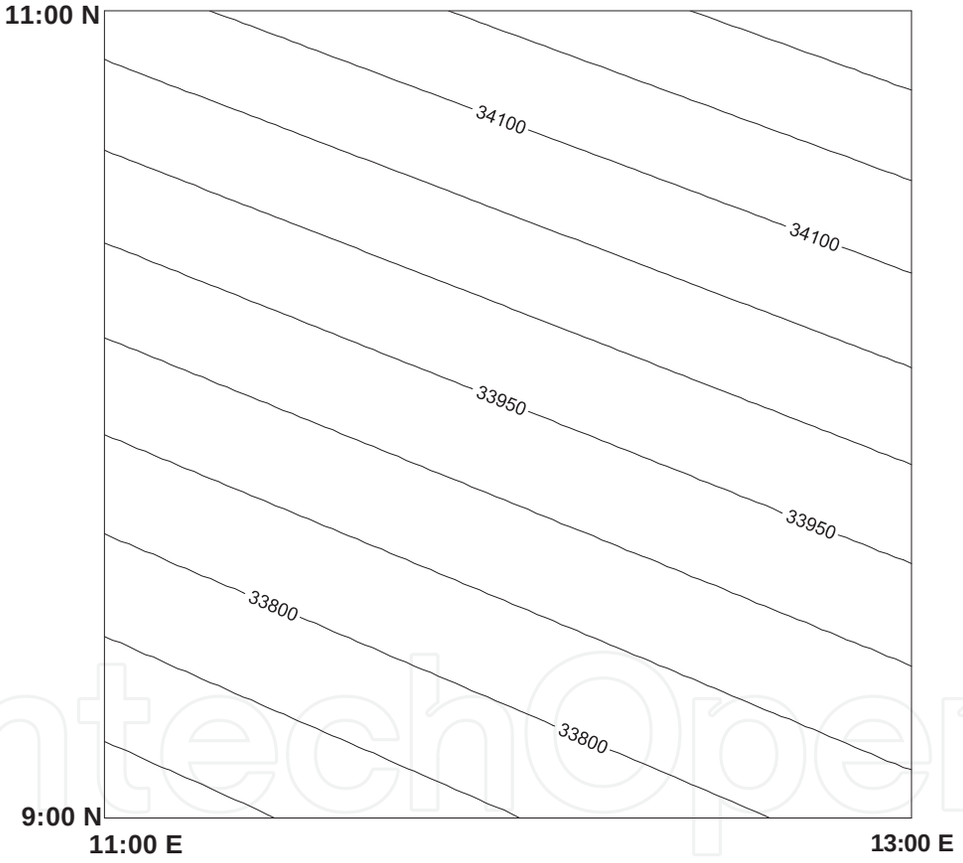

Figure 8. Definitive Geomagnetic Reference Model (DGRF2005) over UBT at 100 m above ground level. The Earth's model used is geodetic and CI is 50 nT.

10.3. Analysis of aeromagnetic field

We have computed for the present study area (UBT) the field, F for the epoch year 2005 and is displayed in contour form (Fig. 8) and because of the relatively small size of the study area, the values of D and I cannot be contoured and imaged. However between these values of

Longitudes and Latitudes (11°E – 13°E, 9°N – 11°N), D ranges from -1.4° (11°E, 9°N) to -0.7° (13°E, 11°N) and I ranges from -5.7° (11°E, 9°N) to -0.2° (13°E, 11°N).

The Definitive Geomagnetic Reference Field (DGRF) or the main field map of the study area (Fig. 8) shows a NW-SE trending lines that have increasing values from the SW portion (minimum value of 33688 nT) to the NE portion (maximum value of 34271 nT) having an average value of 33974 nT and standard deviation of 129 nT. The inclination of the field for this epoch period (2005) decreases correspondingly from -5.7° to -0.2° indicating that slightly north of 11° latitude, the inclination of 0° or magnetic equator passes. We are therefore dealing with a low magnetic latitude area. Similarly the geomagnetic declination varies correspondingly from -1.4° to -0.7° which also shows that further north of 11° latitude, the declination would be 0°, indicating that geomagnetic and geographic meridians coincide. Computations of the rate of change of declination, D (in minutes per year) shows a constant value of 6 minutes/year, rate of change of inclination, I shows a northward increase from -4 to -3 minutes/year and also a northward increase of secular variation in the total field, F of between 21 – 24 nT/year. This shows that beginning 2010, Nigeria will be completely in the southern magnetic hemisphere in the next 40 years, where then the 0° latitude or magnetic equator will be passing through Niger Republic.

The image display of the aeromagnetic total field anomaly map (Fig. 9) has negative anomaly values. This is not surprising and in fact it is expected. The study area and generally Nigeria is situated in a magnetically low-latitude area. The polarizing field of the Earth in such areas is the horizontal component, H. Note that the structure of the Earth' magnetic field resembles that of a bar magnet. At the magnetic poles, the field is essentially vertical (Z), at the centre of the magnetic bar the field is horizontal (H). The horizontal component, H of the total field, F around or at the magnetic equator is therefore the polarizing field. Any magnetically susceptible (non-zero susceptibility) earth materials within this area will be magnetized or polarized by H. When H field induces a polarization field in a susceptible material, the orientation of the field lines describing the magnetic field is rotated 90°. Above this susceptible earth material, the polarization field now points in the opposite direction as the Earth's main field. Thus the total field measured will be less than the Earth's main field, and so upon removal of the main field, the resulting anomalous field will be negative. This is not the case in high-latitude areas, for the same susceptible earth material, where the anomalous field over such would be largely positive and/or negative where also the rotation of the polarizing field depends on the value of inclination, I.

The anomaly map in Figure 9 can be broadly characterized into at least 4 colour zones with the following grid values: -2264 to – 982 nT, -982 to – 877 nT, -877 to -731 nT and -731 to -653 nT running from the NE edge and terminating to the SW side. There appears to be a shear zone running NW-SE nearly bisecting the area and passing through Girei, Shellen, Wuyo and disappearing or being interrupted by Gombe grid probably by reason of an offset NE-SW feature occupying the middle of Gombe grid and pinching out on Biu grid (Fig. 9). The Biu basalts and other high-susceptibility rocks around must have been very influential in the recorded low magnetic anomaly values at NE portion of the map area, particularly towards the northern edges of Bajoga, Gulani, Biu and Chibuk grids.

http://dx.doi.org/10.5772/57163

To demonstrate the usefulness of digital tools in the analysis of magnetic data, we shall apply only one digital processing tool to the analysis of the aeromagnetic total-field anomaly over UBT. We shall use the analytic signal technique.

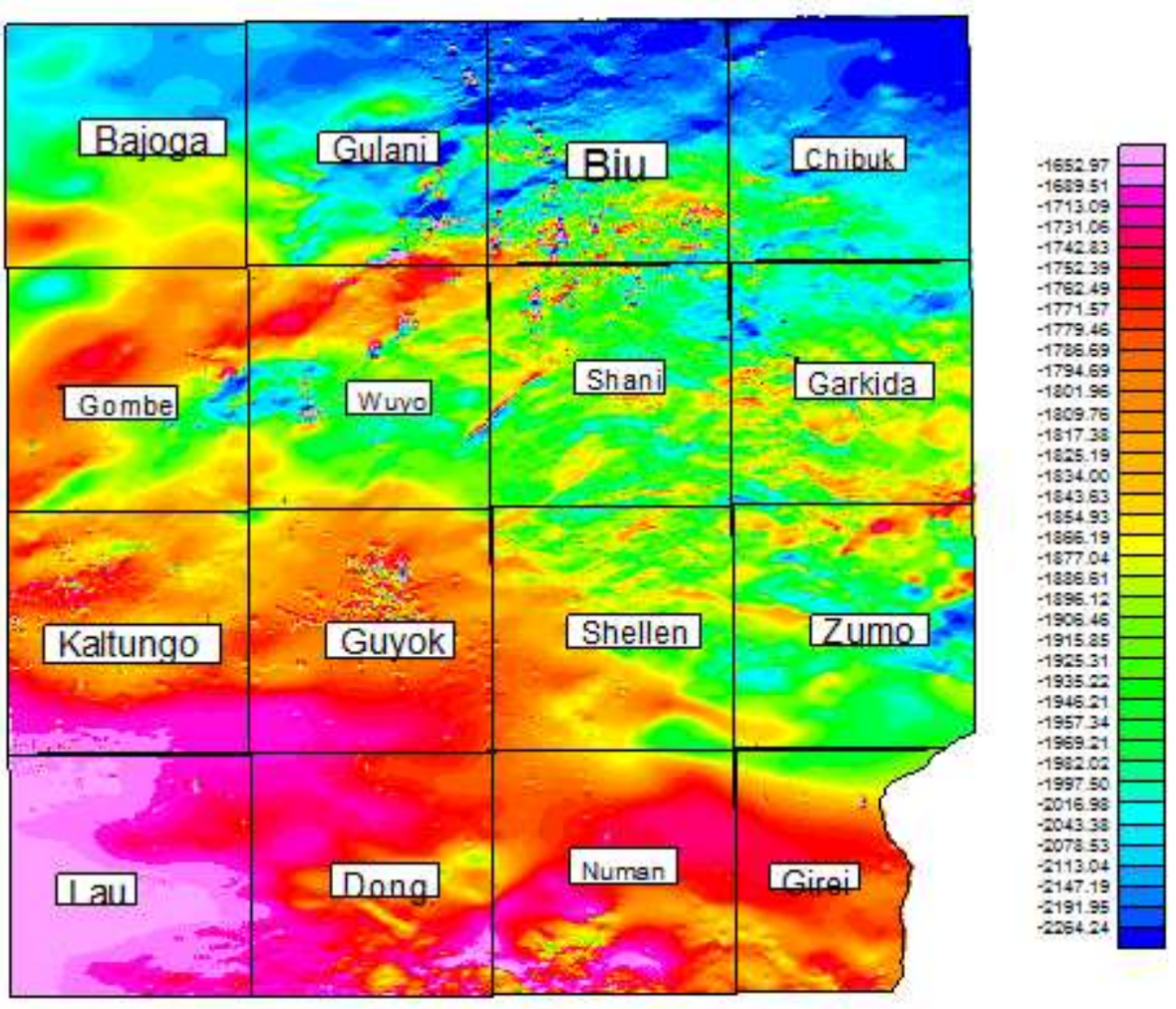

Figure 9. The total-field aeromagnetic anomaly over UBT. A value of 1000 nT should be added to map values.

The analytic signal for magnetic anomalies was initially defined as a 'complex field deriving from a complex potential' [30]. A 3-D analytic signal $\vec{A}$ [43], [53] of a potential field anomaly, M (magnetic field or vertical gradient of gravity), can be defined as:

$$\vec{A}(x,\ y)=\frac{\partial M}{\partial x}\hat{x}+\frac{\partial M}{\partial y}\hat{y}+\frac{\partial M}{\partial z}\hat{z} \tag{24}$$

Where $\hat{x},\ \hat{y},\ \hat{z}$ are unit vectors in the x-, y- and z-axis directions. The analytic signal amplitude or its absolute value can be expressed by a vector addition of the two real components in the x and y directions and of the imaginary component in the z-direction, i.e.

$$|\vec{A}(x,\ y)| = \sqrt{\left(\frac{\partial M}{\partial x}\right)^2 + \left(\frac{\partial M}{\partial y}\right)^2 + \left(\frac{\partial M}{\partial z}\right)^2} \tag{25}$$

The field and the analytic signal derivatives are more easily derived in the wave number domain. If F (M) is the Fourier transform of M in the 2-D wave number domain with wave number $\vec{k} = (k_x,\ k_y)$, the horizontal and vertical derivatives of M correspond respectively to multiplication of F (M) by $i(k_x,\ k_y) = i\vec{k}$ and $|\vec{k}|$. In 3-D the gradient operator in frequency domain is given by $\vec{\nabla} = ik_x\hat{x} + ik_y\hat{y} + |\vec{k}|\hat{z}$. The Fourier transform of the analytic signal can then be expressed in terms of the gradient of the Fourier transform of the field M by the following equation equivalent to the space-domain equation above, i.e. [53]:

$$\hat{t}.F\left(\vec{A}(x,y)\right) = \hat{h}.\vec{\nabla}F(M) + i\hat{z}\vec{\nabla}F(M) \tag{26}$$

Where $\hat{h} = \hat{x} + \hat{y}$ is the horizontal unit vector and $\hat{t} = \hat{h} + \hat{z}$.

The amplitude of the 3-D analytic signal of the total magnetic field anomaly produces maxima over magnetic contacts regardless of the direction of magnetization. The absence of magnetization direction in the shape of analytic signal anomalies is a particularly attractive characteristic for the interpretation of magnetic field near the magnetic latitude like the area under test. It is also known that the depths to sources can be determined from the distance between inflection points of analytic signal anomalies, but have not explored that option and interested readers can refer to [54].

In this method, we have applied the concept of analytic signal to the residual total magnetic field intensity of the UBT. These processes were accomplished by use of Geosoft Oasis Montaj (version 8.0).

Figure 10 shows the output of the analytical signal amplitude calculated from the original total-field magnetic anomaly (Fig. 9). Analytic signal of the total-field magnetic anomaly reduces magnetic data to anomalies whose maxima mark the edges of magnetized bodies and whose shape can be used to determine the depth of these edges (we have not done this second aspect).

The analytic signal amplitude over the UBT ranges from 0.00 nT/m to 7.93 nT/m: having a mean of 0.036 nT/m and standard deviation of 0.073 nT/m. Since amplitude of the analytic signal anomalies combines all vector components of the field into a simple constant, a good way to think of analytic signal is as a map of magnetization in the ground. With this in mind, we can picture strong anomalies to exist over where the magnetization vector intersects magnetic contrasts, even though one cannot know the source of the contrasts from the signal amplitude alone. Consequently, we can easily see the boundaries of the Biu basalts properly demarcated (Fig. 10) shown by the higher analytic signal values. Note also the few scattered imprints of the same basalts tailing to the SW direction from this major anomaly. The Biu area is composed of Tertiary and Quaternary periods (less than 65 Ma ago) basaltic lava flows containing abundant peridotite xenoliths.

http://dx.doi.org/10.5772/57163

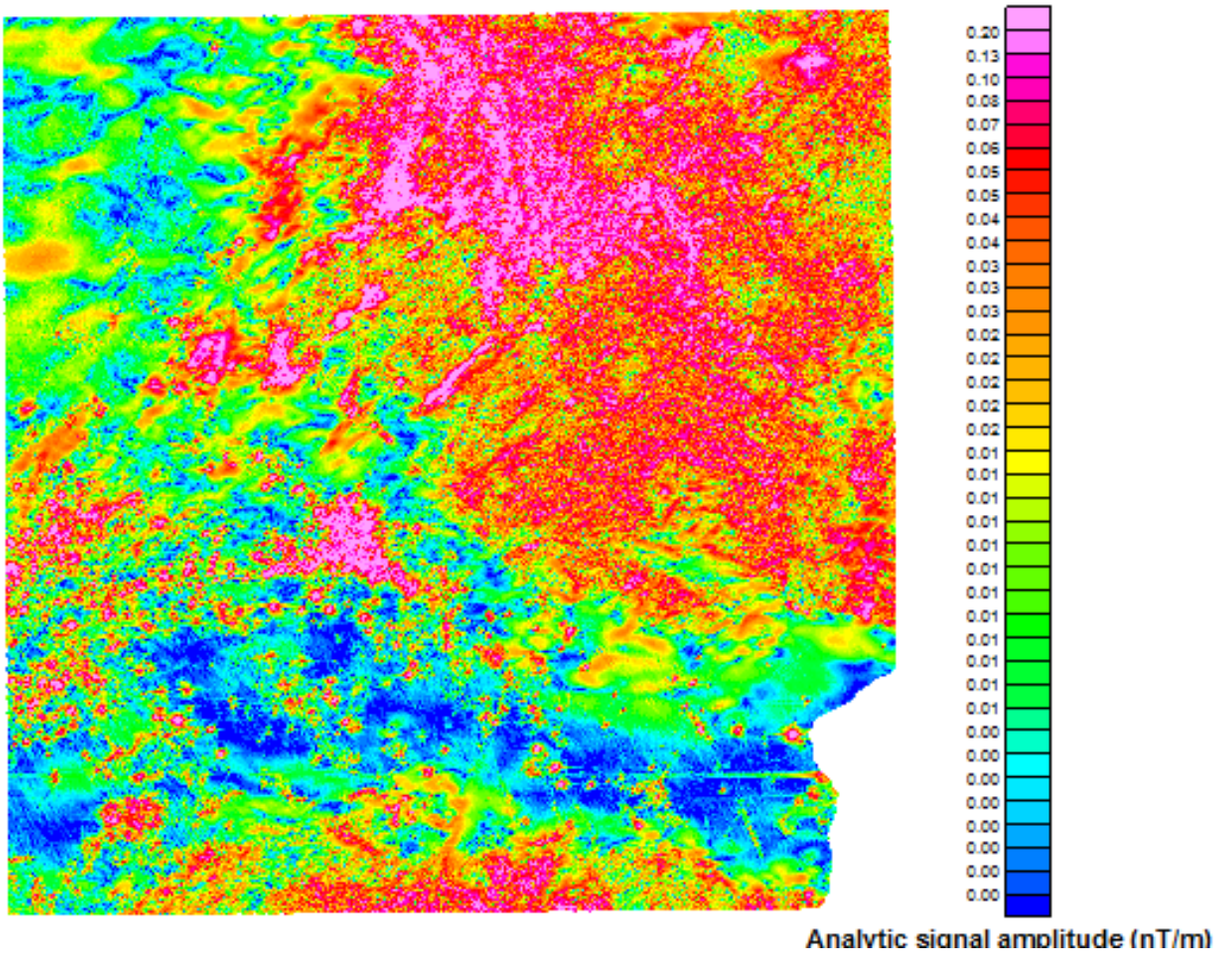

Figure 10. Output of the analytic signal amplitude over UBT. The boundary of high amplitude anomaly over the Biu area (basaltic areas) are delineated

11. Conclusion

In this chapter we have explored the magnetic method for economic exploration of the Earth. The strength of the method lies in the adequate distribution of magnetization within the crustal materials of the Earth in the light of measurable magnetic field over them.

The Earth's magnetic field, that is central in the remanence and induced processes, is itself complex. Spherical harmonic analysis provides the means of characterizing the Earth's magnetic field and with such a representation; it is possible to predict the geomagnetic dipolar field and other non-dipolar components. The knowledge of the dipolar field of the Earth enables the magnetic anomaly to be determined over a survey area from measurements of the magnetic field induction.

We have applied the magnetic method to real field measurements of total-field aeromagnetic intensity data over the Upper Benue Trough, Nigeria. The working data were corrected for secular variation using the existing DGRF model. The anomaly field which is the summary of the crustal field was further processed to obtain the amplitude of analytic signal of the anomaly

field. The analytic signal transformations combine derivative calculations to produce an attribute that is independent of the main inclination and direction of magnetization as well as having peaks over the edges of wide bodies. Thus a simple relationship between the geometry of the causative bodies and the transformed data is observed such as seen in Figure 10. We note that the borders of the Biu basalt as exposed by the applied analytic signal technique of the magnetic anomaly data goes beyond the outcropping boundary that may be offered by remotely sensed data. We recognize that even though the magnetic data were remotely sensed, the result from such measurements goes beyond what the traditional remote sensing information can offer.

The greatest limitation of the magnetic method is the fact that it only responds to variations in the magnetic properties of the earth materials and so many other characteristics of the subsurface (e.g. regolith characteristics) are not resolvable. The inherent ambiguity in magnetic interpretation (for quantitative techniques) is problematic where several geologically plausible models can be attained from the data. Interpreters of magnetic data must therefore be aware of such limitations and be prepared to obtain confirmatory facts from other databases to decrease the level of ambiguity.

Acknowledgements

I acknowledge the National Centre for Petroleum Research and Development (NCPRD), of the Energy Commission of Nigeria (ECN), Abubakar Tafawa Balewa Balewa University, Bauchi, Nigeria for supporting this research.

Author details

Othniel K. Likkason

Physics Programme, Abubakar Tafawa Balewa University, Bauchi, Nigeria

References

[1] Grant, F. S. Aeromagnetics, geology and environments I, magnetite in igneous, sedimentary and metamorphic rocks: an overview. Geoexploration1985; 23 303 - 333

[2] Campbell, W. C. Introduction to geomagnetic fields: Cambridge University Press; 1997

[3] Cox, A. Plate tectonics and geomagnetic reversals. W. H. Freeman and Company; 1973

[4] McElhinny, W. M. Paleomagnetics and plate tectonics: Cambridge University Press; 1973

[5] McElhinny, W. M., McFadden, P. L. Paleomagnetism – continents and oceans: Academic Press; 2000

[6] Merrill, R. T., McElhinny, M. W., McFadden, P. L. Magnetic field of the earth; paleomagnetism, the core and the deep mantle: Academic Press, San Diego;1996

[7] Doell, R., Cox, A. Magnetization of rocks, In: Mining Geophysics Volume 2: Theory, Society of Exploration Geophysicists SEG Mining Geophysics Volume Editorial Committee (Eds.):1967 446-453, Tulsa

[8] Telford, W. M., Geldart, L. P., Sheriff, R. E., Keys, D. A. Applied geophysics. Cambridge University Press, London:1990

[9] Chapman, S., Bartels, J. Geomagnetism. Oxford University Press:1940

[10] Haggerty, S. E. The aeromagnetic mineralogy of igneous rocks. Canadian Journal of Earth Sciences 1979: 16 1281-1293

[11] Reynolds, R. L., Rosenbaum, J. G., Hudson, M. R., Fishman, N. S. Rock magnetism, the distribution of magnetic minerals in Earth's crust and aeromagnetic anomalies. U. S. Geological Survey Bulletin 1990; 1924.24-45.

[12] Clark, D. A. Magnetic petrophysics and magnetic petrology: aids to geological interpretation of magnetic surveys. AGSO Journal of Australian Geology and Geophysics 1997;17.83-103

[13] Clark, D. A., Emerson, D. W. Notes on rock magnetization characteristics in applied geophysical studies. Exploration Geophysics 1991; 22.547-555.

[14] Luyendyk, A. P. J. Processing of airborne magnetic data. AGSO J. Australian Geol. Geophys. 1998;17 31-38

[15] Minty, B. R. S. Simple micro-leveling for aeromagnetic data. Exploration Geophysics 1991;.22.591-592.

[16] Kay, S. M. Fundamentals of statistical signal processing. Prentice Hall, Englewood Cliffs, NJ.; 1993

[17] Naidu, P. S., Mathew, M. P. Analysis of geophysical potential fields. Elsevier Science Publishers, Netherlands; 1998

[18] Blakely, R. J. Potential theory in gravity and magnetic applications. Cambridge University Press; 1996

[19] Baranov, V. A new method for interpretation of aeromagnetic maps: pseudo-gravimetric anomalies. Geophysics 1957:.22.359-383

[20] Grauch, V. J. S., Cordell, L. Limitations on determining density or magnetic boundaries from horizontal gradient of gravity or pseudogravity data. Geophysics 1987: 52.118-121

[21] Grauch, V. J. S. A new variable magnetization terrain correction method for aeromagnetic data. Geophysics 1987: 52 94-107.

[22] Nettleton, L. L. Gravity and magnetic calculations. Geophysics 1942:7.293-310

[23] Talwani, M., Heirtzler, J. M. Computation of magnetic anomalies caused by two-dimensional structures of arbitrary shape, In: Computers in mineral industries, G. A. Parks (Ed.) 464-480, Stanford Univ.: 1964

[24] Talwani, M. Computation with help of a digital computer of magnetic anomalies caused by bodies of arbitrary shape. Geophysics 165: 30 797-817

[25] Bhattacharyya, B. K. Continuous spectrum of the total magnetic field anomaly due to a rectangular prismatic body, Geophysics 1966: 31 97-121

[26] Hjelt, S. Magnetostatic anomalies of dipping prisms. Geoexploration 1972:10, 239-254

[27] Werner, S. Interpretation of magnetic anomalies at sheet-like bodies. Sveriges Geol. Undersok. Ser. C, Arsbok, 1953:43(6)

[28] O'Brien, D. P. CompuDepth: a new method for depth-to-basement computation. Presented at the 42nd Annual International Meeting 1972, SEG.

[29] Naudi, H. Automatic determination of depth on aeromagnetic profiles. Geophysics 1971: 36 717-722

[30] Nabighian, M. N. The analytic signal of two-dimensional magnetic bodies with polygonal cross-section: its properties and use for automated anomaly interpretation. Geophysics 1972:.37 507-517

[31] Nabighian, M. N. Additional comments on the analytic signal of two-dimensional magnetic bodies with polygonal cross-section. Geophysics 1974: 39 85-92

[32] Thompson, D. T. EULDPH – a new technique for making computer-assisted depth estimates from magnetic data. Geophysics 1982: 47 31-37.

[33] Thurston, J. B., Smith, R. S. Automatic conversion of magnetic data to depth, dip and susceptibility contrast using the SPI ™ method. Geophysics 1997: 62.807-813

[34] Spector, A., Grant, F. S. Statistical models for interpreting aeromagnetic data. Geophysics 1970: 35 293-302

[35] Cordell, L., McCafferty, A. E. A terracing operator for physical property mapping with potential field data. Geophysics 1989: 54 621-634.

[36] Grant, F. S. The magnetic susceptibility mapping method for interpreting aeromagnetic survey:43rd Annual International Meeting, SEG 1973 expanded abstract 1201.

[37] Pedersen, L. B.Interpretation of potential field data – a generalized inverse approach. Geophysical Prospecting, 1977: 25 199-230.

[38] Pilkington, M. & Crossley, D. J. Inversion of aeromagnetic data for multilayered crustal models. Geophysics 1986: 51 2250-2254.

[39] Pustisek, A. M. Noniterative three-dimensional inversion of magnetic data. Geophysics 1990:55 782-785.

[40] Li, Y. & Oldenburg, D. W. 3-D inversion of magnetic data. Geophysics 1996:61 394-408.

[41] Shearer, S. & Li, Y. 3 D inversion of magnetic total gradient in the presence of remanent magnetization. 74th Annual International Meeting, SEG 2004: Abstracts 774-777

[42] Kellogg, O. D. Foundations of potential field theory. Dover New York; 1953

[43] Nabighian, M. N. Toward a three dimensional automatic interpretation of potential field data via generalized Hilbert transforms: fundamental relation,.Geophysics 1984:49 957-966

[44] Spector, A. Spectral analysis of aeromagnetic data. Ph.D thesis, University of Toronto; 1968

[45] Moreau, F. D. G., Holschneider, M., Saracco, G. Wavelet analysis of potential fields. Inverse Problems 1997:13 165-178

[46] Pelton, C. A computer program for hill-shading digital topographic data sets. Computers and Geosciences 1987:13 545-548.

[47] Rajagopalan, S., Milligan, P. Image enhancement of aeromagnetic data using automatic gain control. Exploration Geophysics 1995: 25 173-178.

[48] Dentith, M., Cowan, D. R., Tompkins, L. A. Enhancement of subtle features in aeromagnetic data. Exploration Geophysics 2000:31 104-108

[49] Carter, J. D., Barber, W., Tait, E. A., Jones, G. P. The geology of parts of Adamawa, Bauchi and Bornu provinces in northeastern Nigeria. Bull. Geol. Survey Nigeria 1963:30 p108

[50] Cratchley, C. R. & Jones, G. P. An interpretation of the geology and gravity anomalies of the Benue Valley, Nigeria, Overseas Geological Surveys, Geophysical Paper 1965 (1)

[51] Burke, K., Dessauvagie, T. F. J., Whiteman, A. J. Geological history of the Benue Valley and adjacent areas, In: African Geology, T. F. J. Dessauvagie & A. J. Whiteman (Eds.) University of Ibadan Press, Nigeria; 1970

[52] Benkhelil, M. J. The origin and evolution of the Cretaceous Benue Trough, Nigeria, Journal of African Earth Sciences 1989: 8 251-282

[53] Roest, W. R., Verhoef, J., Pilkington, M. Magnetic interpretation using 3-D analytic signal. Geophysics 1992: 57 116-125

[54] Debeglia, N. & Corpel, J. Automatic 3-D interpretation of potential field data using analytic signal derivatives. Geophysics 1997:62 87-96

IntechOpen